# Supplementary Material to the paper "Deconstructing the core dynamics from a complex time-lagged regulatory biological circuit", *Eriksson et al.*

## S1 Model reduction process

### S1.1 Dynamical analysis of the original NT-model

**Identification of variable dependencies.** A directed graph (Fig. S1$a$) was constructed to describe the dependencies between the variables of the NT-model (1)-(17). The NT-variables are, in principle (see Fig. S1$a$), represented by nodes in this graph, and there is an edge from node $j$ to $i$ if $j$ is on the right hand side of an equation defining $i$. Arrows $i \to i$ are not illustrated.

For further use, we also introduce two *auxiliary variables*

$$\text{Tri13} = ([\text{Cdc13}_\text{T}] - [\text{Trimer}])/[\text{Cdc13}_\text{T}] \tag{S1}$$

$$\text{SlpSte} = k_2''[\text{Ste9}] + k_2'''[\text{Slp1}]. \tag{S2}$$

where [Trimer] is given in equations (10) and (15). Note that with the introduction of Tri13, equation (11) can be written

$$[\text{MPF}] = ([\text{Cdc13}_\text{T}] - [\text{preMPF}])\text{Tri13}. \tag{S3}$$

**Steady-state behaviour of each variable as a function of its closest neighbours** The steady-state behaviour of the variables of the NT-model can be represented by *steady-state input/output functions* $f^{ss}$. Let $x_i$ be a variable corresponding to one node in the graph of Fig. S1*a*, further, let $u_i^1, u_i^2, ...$ be the input variables to that node, e. g. for the node corresponding to $[\text{Rum1}_\text{T}]$, $x_{[\text{Rum1}_\text{T}]} = [\text{Rum1}_\text{T}]$ and $u^1_{[\text{Rum1}_\text{T}]} = [\text{MPF}], u^2_{[\text{Rum1}_\text{T}]} = [\text{SK}]$. The dynamics of each variable of the graph of Fig. S1*a* is described by a differential equation $\dot{x_i} = g_i(x_i, u_i^1, u_i^2, ...)$ (corresponding to equations (1-9) of the original NT-model), or an algebraic equation $x_i = h_i(u_i^1, u_i^2, ...)$ (corresponding to equations (11-14) of the original NT-model and the introduced auxiliary variables (S1,S2) ). The steady-state of the variable $x_i$ is defined by the *steady-state input/output function* $x_i = f_i^{ss}(u_i^1, u_i^2, ...)$, which is derived from the differential equations (1-8) by solving the equation $g_i(x_i, u_i^1, u_i^2, ...) = 0$

for $x_i$, or, in the case of the algebraic equations (i. e. equations (11)-(14) and (S1,S2)) given directly, $f_i^{ss} = h_i(u_i^1, u_i^2, ...)$, (see also [1]). Notably, the equation $g_i(x_i, u_i^1, u_i^2, ...) = 0$ seam to have an unique solution for all NT-variables, in the considered range, under biological conditions. Biological conditions is defined by [IEP] $\leq 1$, [PreMPF] $\leq$ [Cdc13$_{\mathrm{T}}$], [Slp1] $\leq$ [Slp1$_{\mathrm{T}}$], [Ste9] $\leq 1$ and all variables satisfy $\geq 0$. For each variable the steady-state input/output function $f_i^{ss}(u_i^1, u_i^2, ...)$, was retrieved, analytically or numerically using *Mathematica* (http://www.wolfram.com/). For differential equations (3) and (6) the biological steady-state solution correspond to the Goldbeter-Koshland equation [2, 1, 3].

**Steady-state behaviour of subsets of variables.** Next we observe that we can retrieve steady-state functions for subsets of variables by successive variable elimination. As an example, consider the subset consisting of the original NT-variables $\{[\mathrm{Slp1}], [\mathrm{Slp1_T}], [\mathrm{IEP}]\} = M_{\mathrm{slp}}$, see Fig. S1*a*. At steady-state this subset can be considered as a single unit with input [MPF] and output [Slp1]. We earlier noted that the steady-state dependence of the variables on their closest neighbors could be described by uniquely defined functions. For [Slp1] this function corresponds to $[\mathrm{Slp1}] = f^{ss}_{[\mathrm{Slp1}]}(u^1_{[\mathrm{Slp1}]}, u^2_{[\mathrm{Slp1}]}) = f^{ss}_{[\mathrm{Slp1}]}([\mathrm{Slp1_T}], [\mathrm{IEP}])$ and for [Slp1$_{\mathrm{T}}$] and [IEP] to $[\mathrm{Slp1_T}] = f^{ss}_{[\mathrm{Slp1_T}]}([\mathrm{MPF}])$ and $[\mathrm{IEP}] = f^{ss}_{[\mathrm{IEP}]}([\mathrm{MPF}])$. The subset $M_{\mathrm{slp}}$ with input [MPF] and output [Slp1] can thus be described by the steady-state function

$$[\mathrm{Slp1}] = f^{ss}_{[\mathrm{Slp1}]}(f^{ss}_{[\mathrm{Slp1_T}]}([\mathrm{MPF}]), f^{ss}_{[\mathrm{IEP}]}([\mathrm{MPF}])) = f^{ss}_{M_{\mathrm{Slp}}}([\mathrm{MPF}]). \qquad \text{(S4)}$$

The steady-state behaviour of the subset $\{[\mathrm{SK}], [\mathrm{TF}]\} = M_{\mathrm{sk}}$, see Fig. S1*a*, with input $[\mathrm{MPF}], \mathrm{M}$ and output [SK] can be retrieved in a similar way

$$[\mathrm{SK}] = f^{ss}_{[\mathrm{SK}]}(f^{ss}_{[\mathrm{TF}]}([\mathrm{MPF}], \mathrm{M})) = f^{ss}_{M_{\mathrm{sk}}}([\mathrm{MPF}], \mathrm{M}). \tag{S5}$$

## S1.2 Construction of reduced model

### S1.2.1 Defining dynamical switching modules

From dynamical dependencies between the variables we defined switching modules (Fig. S1) that were approximated by step-functions. These modules are subsets of variables chosen so that i) the variables within a subset are *connected*, ii) the group has only *one output* that needs to be recorded and iii) this output has a *switching input/output behaviour*. A switching input/output behaviour is loosely defined as a steep "sigmoidish" steady-state input/output curve, see Figures S2-S5. Furthermore, if the input to a potential switching module comes from an already defined switching module, then this input is considered as binary (high or low) and only two values have to be tested when considering iii) above. With this strategy we defined the following switching modules $M_{25} = \{k_{25}\}$, $M_{\mathrm{wee}} = \{k_{\mathrm{wee}}\}$, $M_{\mathrm{slp}} = \{[\mathrm{IEP}], [\mathrm{Slp1_T}], [\mathrm{Slp1}]\}$, $M_{\mathrm{sk}} = \{[\mathrm{TF}], [\mathrm{SK}]\}$, $M_{\mathrm{ste}} = \{[\mathrm{Ste9}]\}$ $M_{\mathrm{rum}} = \{[\mathrm{Rum1_T}]\}$ and $M_{\mathrm{tri}} = \{\mathrm{Tri13}\}$, as indicated in Fig. S1*a*.

### S1.2.2 Delayed step-function approximations

The dynamical behaviour of the subsets were approximated by step-functions with time delay. With this approximation, the remaining system, i.e. the dynamics of the variables [$\mathrm{Cdc13_T}$], [PreMPF] and [MPF] turns out to be piecewise linear.

To estimate the parameters of the time-delayed step-functions two methods were used. i) The high $h_i$, low $l_i$ and threshold $\theta_i$ parameters of the step-functions were tentatively estimated from the corresponding steady-state input/output functions $f_i^{ss}$ of the original NT-model, Figures S2-S5, and fine-tuned from comparison of full scale numerical simulations between the NT- and DPL-model. ii) The delay parameters $\tau_i$ were tentatively estimated from the input/output response of the modules of the NT-model, to a stepwise changing input Fig. S6 and fine-tuned from full scale numerical simulations.

If an input $u$ to a switching module came from another switching module which had already been approximated by a step-function, the input $u$ was considered as binary ($u \in \{h, l\}$). Further more, in order to get a simple description some switching thresholds of the original NT-model were ignored in the formulation of the DPL-model as described below.

**Tentative estimation of parameters $h_i$, $l_i$ and $\theta_i$:**

*Subsystems $M_{25}, M_{\mathrm{wee}}$ and $M_{\mathrm{slp}}$:*

The steady-state input/output functions $f_i^{ss}$ of these subsystems (solid lines Fig. S2) corresponds to $k_{25} = f_{k_{25}}^{ss}([\mathrm{MPF}])$ (equation (14)), $k_{\mathrm{wee}} = f_{k_{\mathrm{wee}}}^{ss}([\mathrm{MPF}])$

(equation (13)) and $f^{ss}_{M_{\rm slp}}([\text{MPF}])$ (equation (S4)) respectively. These functions were approximated by the step-functions $s_{25}$, $s_{\rm wee}$ and $s_{\rm slp}$

$$s_{25}(mpf) = \begin{cases} l_{25} & \text{if } mpf \leq \theta_{25} \\ h_{25} & \text{if } mpf > \theta_{25} \end{cases}, \tag{S6}$$

$$s_{\rm wee}(mpf) = \begin{cases} h_{\rm wee} & \text{if } mpf \leq \theta_{\rm wee} \\ l_{\rm wee} & \text{if } mpf > \theta_{\rm wee} \end{cases}, \tag{S7}$$

$$s_{\rm slp}(mpf) = \begin{cases} l_{\rm slp} & \text{if } mpf \leq \theta_{\rm slp} \\ h_{\rm slp} & \text{if } mpf > \theta_{\rm slp} \end{cases}, \tag{S8}$$

dashed lines Fig. S2. The high $h_i$ and low $l_i$ values $i \in \{25, \text{wee}, \text{slp}\}$ in the step-functions correspond to the maximum and minimum of the corresponding functions$f^{ss}_{k_{25}}([\text{MPF}])$, $f^{ss}_{k_{\rm wee}}([\text{MPF}])$ and $f^{ss}_{M_{\rm slp}}([\text{MPF}])$ when $[MPF] \geq 0$. The threshold $\theta_i$ corresponds to the value of [MPF] for which
$f^{ss}_i([\text{MPF}] = \theta_i) = l_i + (h_i - l_i)/2$.

*Subsystem $M_{\rm sk}$:*

The subsystem $M_{\rm sk}$ is approximated by the step-function $s_{\rm sk}$,

$$s_{\rm sk}(mpf, M) = \begin{cases} h_{\rm sk} & \text{if } \phi' mpf + \phi'' M \leq \theta_{\rm sk} \\ l_{\rm sk} & \text{if } \phi' mpf + \phi'' M > \theta_{\rm sk} \end{cases}, \tag{S9}$$

constructed from the steady-state function $f^{ss}_{M_{\rm sk}}([\text{MPF}], \text{M})$ (equation (S5),

Fig. S3$a$) according to $h_{\mathrm{sk}} = \max(f^{ss}_{M_{\mathrm{sk}}}([\mathrm{MPF}], \mathrm{M}))$ and $l_{\mathrm{sk}} = \min(f^{ss}_{M_{\mathrm{sk}}}([\mathrm{MPF}], \mathrm{M}))$, $([\mathrm{MPF}], \mathrm{M} \geq 0)$. The threshold corresponds to the values of [MPF] and M for which $f^{ss}_{M_{\mathrm{sk}}}([\mathrm{MPF}], \mathrm{M}) = l_i + (h_i - l_i)/2$. We approximated this threshold from Fig. S3$a$ with the line $\phi'[\mathrm{MPF}] + \phi''\mathrm{M} = \theta_{\mathrm{sk}}$.

*Subsystem $M_{\mathrm{ste}}$:*

The step-function $s_{\mathrm{ste}}$ is approximated from the steady-state input/output function $f^{ss}_{[\mathrm{Ste9}]}([\mathrm{MPF}], [\mathrm{Slp1}], [\mathrm{SK}])$, see Fig. S4. The high value corresponds to the maximum, $h_{\mathrm{ste}} = \max(f^{ss}_{[\mathrm{Ste9}]}([\mathrm{MPF}], [\mathrm{Slp1}], [\mathrm{SK}]))$, and the low value to the minimum, $l_{\mathrm{ste}} = \min(f^{ss}_{[\mathrm{Ste9}]}([\mathrm{MPF}], [\mathrm{Slp1}], [\mathrm{SK}]))$, $([\mathrm{MPF}], [\mathrm{Slp1}], [\mathrm{SK}] \geq 0)$. To find the switching threshold in the three variable input-space we use the fact that the variables [Slp1] and [SK] earlier were approximated by the step-functions $s_{\mathrm{slp}} \in \{h_{\mathrm{slp}}, l_{\mathrm{slp}}\}$ and $s_{\mathrm{sk}} \in \{h_{\mathrm{sk}}, l_{\mathrm{sk}}\}$. The threshold can thus be constructed from the four possible combinations of $h_{\mathrm{slp}}, l_{\mathrm{slp}}$ and $h_{\mathrm{sk}}, l_{\mathrm{sk}}$ (Fig S4). We have noted that the switch when input [Slp1] $= h_{\mathrm{slp}}$ ([MPF] $\approx 0.9$, upper two graphs of Fig. S4) is not necessary to mimic the behaviour of the wild-type cell. Therefore, in order to simplify the model we have ignored this switch. When [MPF] $> 0.8$ we "extrapolate" the behaviour of [MPF] $< 0.8$ and discard the switch when [MPF] $\approx 0.9$. This leads to the

following step-function

$$s_{\text{ste}}(mpf, slp1, sk) = \begin{cases} h_{\text{ste}} & \text{if } slp1 = h_{\text{slp}} \\ & \text{or } (slp1 = l_{\text{slp}}, sk = l_{\text{sk}} \text{ and } mpf \leq \theta_{\text{ste}}) \\ l_{\text{ste}} & \text{else} \end{cases}, \tag{S10}$$

where $\theta_{\text{ste}}$ corresponds to the threshold retrieved from the function $f^{ss}_{[\text{Ste9}]}([\text{MPF}], [\text{Slp1}] = l_{\text{slp}}, [\text{SK}] = l_{\text{sk}})$ (lower right graph of Fig. S4).

*Subsystem $M_{\text{rum}}$:*

The step-function $s_{\text{rum}}$ was approximated from the original steady-state input/output function $f^{ss}_{[\text{Rum1}_\text{T}]}([\text{MPF}], [\text{SK}])$, in the same way as for [Ste9], i.e. $h_{\text{rum}} = \max(f^{ss}_{[\text{Rum1}_\text{T}]}([\text{MPF}], [\text{SK}]))$, $l_{\text{rum}} = \min(f^{ss}_{[\text{Rum1}_\text{T}]}([\text{MPF}], [\text{SK}]))$, $([\text{MPF}], [\text{SK}] \geq 0)$ and the switching threshold is estimated based on that input [SK] earlier was approximated by $s_{\text{sk}} \in \{h_{\text{sk}}, l_{\text{sk}}\}$, Fig. S5. When estimating the switching threshold we only considered the case when $[\text{SK}] = l_{\text{sk}}$ (left panel Fig. S5) and therefore $\theta_{\text{rum}}$ is retrieved by solving $f^{ss}_{[\text{Rum1}_\text{T}]}([\text{MPF}], [\text{SK}] = l_{\text{sk}}) = l_{\text{rum}} + (h_{\text{rum}} - l_{\text{rum}})/2$ for [MPF]. We approximate the case $[\text{SK}] = h_{\text{sk}}$ (right panel Fig. S5) as $s_{\text{rum}} = l_{\text{rum}} = 0$, yielding the following step-function

$$s_{\text{rum}}(mpf, sk) = \begin{cases} h_{\text{rum}} & \text{if } (sk = l_{\text{sk}} \text{ and } mpf \leq \theta_{\text{rum}}) \\ l_{\text{rum}} & \text{else} \end{cases}. \tag{S11}$$

*Subsystem $M_{\text{tri}}$:*

When [Rum1$_{\text{T}}$] is approximated by $s_{\text{rum}} \in \{l_{\text{rum}} = 0, h_{\text{rum}} = 10\}$ (from Fig. S5*a*), then Tri13 = 1 or Tri13 $\approx$ 0 and we have the following step-function

$$s_{\text{tri13}}(rum1t) = \begin{cases} h_{\text{tri13}} & \text{if } rum1t = l_{\text{rum}} \\ l_{\text{tri13}} & \text{else} \end{cases}, \tag{S12}$$

where $h_{\text{tri13}} = 1$ and $l_{\text{tri13}} = 0$.

**Tentative estimation of parameters** $\tau_i$ The transient time of the subsystems $M_{\text{slp}}, M_{\text{sk}}, M_{\text{rum}}$ and $M_{\text{ste}}$ was measured by examining the step-response to different input, Fig. S6 (The subsystems $M_{25}$, $M_{\text{wee}}$ and $M_{\text{tri}}$ have an immediate response by definition.). For subsystems with more than one input, the inputs were tested one at a time, keeping the other at a constant value. Inspection of the graphs of Fig. S6 gave tentative estimates of the time-delays of the step-functions. For simplicity, the time delays of $M_{\text{sk}}$ (input $M$), $M_{\text{ste}}$ (all input) and $M_{\text{rum}}$(all input) (Fig. S6 b,d-h) were set to $\tau_i = 0$, since we found that the transient time of these subsystems did not effect on achieving behaviour.

**Fine-tuning of parameters** The parameters were fine-tuned from comparisons between DPL- and NT-model simulations. Two versions of the original NT-model were used in this comparison, the parameter set of the *wild-type*

*cell* (found in (18)) and the $Wee1^{-}$ mutation (parameters (18), except that $k''_{wee} = 0.3$). From this comparison, $l_{25}$ was changed to $l_{25} = 0.2$, as compared to tentative parameter value 0.05, and $\theta_{\text{rum}}$ was changed to $\theta_{\text{rum}} = 0.02$. The delay parameters were designated $\tau_1 = 15$, for the subset $M_{\text{slp}}$, and $\tau_2 = 7$, for the subset $M_{\text{sk}}$ with input [MPF]. All other tentative delays (Fig. S6) were set to zero (see the discussion in the section before). The final set of DPL-model parameters is given in (S13).

### S1.2.3 Full DPL-model ($M \geq 0$)

The discussion above yields the DPL-model corresponding to the full NT-model. Using the notation that $s$ corresponds to step-functions or combinations of step-functions, $x$ variables which remained unmodified during the reduction process, and $y$ denotes [MPF], we have

$$
\begin{aligned}
\dot{x}_{\mathrm{Cdc13_T}}(t) =& - s_1(t, t-\tau_1, t-\tau_2) x_{\mathrm{Cdc13_T}}(t) + k_1 M(t), \\
\dot{x}_{\mathrm{PreMPF}}(t) =& s_2(t) x_{\mathrm{Cdc13_T}}(t) - s_3(t, t-\tau_1, t-\tau_2) x_{\mathrm{PreMPF}}(t), \\
y_{\mathrm{MPF}}(t) =& s_{tri}(t, t-\tau_2)(x_{\mathrm{Cdc13_T}}(t) - x_{\mathrm{PreMPF}}(t)),
\end{aligned}
$$

$$
\begin{aligned}
s_1(t, t-\tau_1, t-\tau_2) =& k_2' + k_2'' s_{\mathrm{ste}}(y_{\mathrm{MPF}}(t), s_{\mathrm{slp}}(y_{\mathrm{MPF}}(t-\tau_1)), s_{\mathrm{sk}}(y_{\mathrm{MPF}}(t-\tau_2), M(t))) \\
& + k_2''' s_{\mathrm{slp}}(y_{\mathrm{MPF}}(t-\tau_1)), \\
s_2(t) =& s_{\mathrm{wee}}(y_{\mathrm{MPF}}(t)), \\
s_3(t, t-\tau_1, t-\tau_2) =& s_{\mathrm{wee}}(y_{\mathrm{MPF}}(t)) + s_{25}(y_{\mathrm{MPF}}(t)) \\
& + k_2' + k_2'' s_{\mathrm{ste}}(y_{\mathrm{MPF}}(t), s_{\mathrm{slp}}(y_{\mathrm{MPF}}(t-\tau_1)), s_{\mathrm{sk}}(y_{\mathrm{MPF}}(t-\tau_2), M(t))) \\
& + k_2''' s_{\mathrm{slp}}(y_{\mathrm{MPF}}(t-\tau_1)), \\
s_{tri}(t, t-\tau_2) =& s_{tri}(s_{\mathrm{rum}}(y_{\mathrm{MPF}}(t), s_{\mathrm{sk}}(y_{\mathrm{MPF}}(t-t_2), M(t)))),
\end{aligned}
$$

$$
\begin{aligned}
\dot{\mathrm{M}}(t) =& \mu \mathrm{M(t)}, \\
& \text{when } y_{MPF} \text{ decreases through } 0.1, \text{ M is divided by two,}
\end{aligned}
$$

where

$$s_{25}(mpf) = \begin{cases} l_{25} & \text{if } mpf \leq \theta_{25} \\ h_{25} & \text{if } mpf > \theta_{25} \end{cases},$$

$$s_{\text{wee}}(mpf) = \begin{cases} h_{\text{wee}} & \text{if } mpf \leq \theta_{\text{wee}} \\ l_{\text{wee}} & \text{if } mpf > \theta_{\text{wee}} \end{cases},$$

$$s_{\text{slp}}(mpf) = \begin{cases} l_{\text{slp}} & \text{if } mpf \leq \theta_{\text{slp}} \\ h_{\text{slp}} & \text{if } mpf > \theta_{\text{slp}} \end{cases},$$

$$s_{\text{sk}}(mpf, M) = \begin{cases} h_{\text{sk}} & \text{if } \phi' mpf + \phi'' M \leq \theta_{\text{sk}} \\ l_{\text{sk}} & \text{if } \phi' mpf + \phi'' M > \theta_{\text{sk}} \end{cases},$$

$$s_{\text{ste}}(mpf, slp1, sk) = \begin{cases} h_{\text{ste}} & \text{if } slp1 = h_{\text{slp}} \\ & \text{or } (slp1 = l_{\text{slp}}, sk = l_{\text{sk}} \text{ and } mpf \leq \theta_{\text{ste}}) \\ l_{\text{ste}} & \text{else} \end{cases},$$

$$s_{\text{rum}}(mpf, sk) = \begin{cases} h_{\text{rum}} & \text{if } (sk = l_{\text{sk}} \text{ and } mpf \leq \theta_{\text{rum}}) \\ l_{\text{rum}} & \text{else} \end{cases},$$

$$s_{\text{tri13}}(rum1t) = \begin{cases} h_{\text{tri13}} & \text{if } rum1t = l_{\text{rum}} \\ l_{\text{tri13}} & \text{else} \end{cases}.$$

Here the parameters are

$$\begin{array}{cccccc} \tau_1 = 15 & \tau_2 = 7 & k_1 = 0.03 & k_2' = 0.03 & k_2'' = 1 & k_2''' = 0.1 \\ l_{25} = 0.2 & h_{25} = 5 & \theta_{25} = 0.25 & h_{\text{wee}} = 1.3 & l_{\text{wee}} = 0.15 & \theta_{\text{wee}} = 0.25 \\ l_{\text{slp}} = 0 & h_{\text{slp}} = 3 & \theta_{\text{slp}} = 0.4 & h_{sk} = 1 & l_{sk} = 0 & \phi' = 1 \\ \phi'' = -0.75 & \theta_{sk} = 0.5 & l_{\text{ste}} = 0 & h_{\text{ste}} = 0 & \theta_{\text{ste}} = 0.029 & h_{\text{rum}} = 10 \\ l_{\text{rum}} = 0 & \theta_{rum} = 0.02 & h_{tri} = 1 & l_{tri} = 0 & \mu = 0.005 & \end{array} \tag{S13}$$

Note that, by the reduction process, these parameters are not all independent.

### S1.2.4 Small DPL-model (M>0.8)

From the inspection of steady-state input/output graphs of subsets of variables (data not shown), we found that the main effect of $M_{\mathrm{sk}} = \{[TF], [SK]\}$, on [Rum1$_{\mathrm{T}}$] and [Ste9] is when $M < 0.8$. The smaller DPL-model (19)-(29), used in the mathematical analysis, make use of this observation. The small DPL-model can be retrieved from the full model by replacing the dynamics of $s_{\mathrm{sk}}$, with a constant parameter $s_{\mathrm{sk}} = h_{\mathrm{sk}} = 1$. Then $s_{\mathrm{rum}} = l_{\mathrm{rum}} = 0$ and $s_{tri} = h_{tri} = 1$, and the dynamics of $s_{\mathrm{ste}}$ is simplified so that it follows the switching behaviour of $s_{\mathrm{slp}}$ (it is on when $s_{\mathrm{slp}}$ is on and off when $s_{\mathrm{slp}}$ is off ). We therefore merge $s_{\mathrm{slp}}$ and $s_{\mathrm{ste}}$ into $s_{\mathrm{slp/ste}}$ (equation (27)) whose dynamics corresponds to $k_2''$[Ste9] + $k_2'''$[Slp1] = SlpSte in the NT-model (equation S2). In Fig. S1*b* variables which have been replaced by constant parameters are indicated by crosses. With this removal of variables, we can define new switching modules (Fig. S1*b*).

## S2 Mutations

The large DPL-model was used in a comparison with the NT-model for different parameter sets corresponding to different mutations. The different parameter sets are displayed in Table S1.

## S3 Comparison between simulations of the NT-model and the small DPL-model for different initial conditions.

Using the original NT-model, (1)-(18), 12 distinct sets of random initial values were designed, each set starting a single simulation. The first $\tau = 15$ minutes of these simulations were then translated to give corresponding sets of initial functions $\mathbf{x}(t) = \mathbf{f}_0(t)$, $t_0 - \tau \leq t < t_0$ of the small DPL-model.

We ensured that the first $\tau = 15$ min of the 12 simulations of the NT-model satisfied the biological constraints $x \geq 0$ for all variables $x$, and [PreMPF] $\leq$ [Cdc13$_{\mathrm{T}}$], [IEP] $\leq 1$,[Ste9] $\leq 1$, [Slp1] $\leq$ [Slp1$_{\mathrm{T}}$], and also that the sets did not include the region M $< 0.8$ for which the small DPL-model was not constructed.

Since the dynamics of [SK] and [Rum1$_{\mathrm{T}}$] were not included when constructing the small DPL-model, these variables were initiated with the starting values [Rum1$_{\mathrm{T}}$]$(t_0 - \tau) = 0$ and [SK]$(t_0 - \tau) = 1$ in all NT-model random sets. The simulations are illustrated in Figures S7-S9. The initial value sets can be received from the corresponding author upon request.

## S4 Proof of theorem on stability

We first prove that there exists a globally stable limit cycle when $M = 1.8$ (lemma 4). For this we need lemma 1-3. Finally, in the end of this section

we expand this proof to all $0.8 < M < 3$.

Let $t_0$ denote the initial time $t_0 = 0$. For $t = t_0$, let $t' \geq 0$ denote the time period since the last time $S^D$ was passed, i.e. $\mathbf{x}(t_0 - t') \in S^D$ and $\mathbf{x}(t_0 - t) \notin S^D, t < t'$. Further on let a *starting scenario*, be a point $\mathbf{x}(t_0)$ together with a time $t'$. We can then divide all starting scenarios that satisfy the restriction on $f_0$ into four groups, $S_1$-$S_4$ (Fig. 7), depending on whether $\mathbf{x}(t_0) \in D1 \cup D2$ or $D3$ and whether $t' < \tau$ or $t' > \tau$.

$$\begin{aligned} S_1: &\quad \mathbf{x}(t_0) \in D1 \cup D2, \quad t' \geq \tau \\ S_2: &\quad \mathbf{x}(t_0) \in D3, \quad t' \leq \tau \\ S_3: &\quad \mathbf{x}(t_0) \in D3, \quad t' > \tau \\ S_4: &\quad \mathbf{x}(t_0) \in D1 \cup D2, \quad t' < \tau \end{aligned} \tag{S14}$$

**Lemma 1.** *At each point* $\mathbf{x}(t_0)$ *in one of the starting scenarios only one linear system can be used, namely*

$$\begin{aligned} S_1: &\quad D1 : \mathbf{A}_{11}\ (S/G2) \quad D2 : \mathbf{A}_{21}\ (M) \\ S_2: &\quad D3 : \mathbf{A}_{21}\ (M) \\ S_3: &\quad D3 : \mathbf{A}_{22}\ (EM) \\ S_4: &\quad D1 : \mathbf{A}_{12}\ (G1) \quad D2 : \mathbf{A}_{22}\ (EM). \end{aligned} \tag{S15}$$

*(The corresponding vector fields of the slow eigenvector approximation are shown in Fig. 7.)*

*Proof:* $S_1$: If $\mathbf{x}(t_0) \in D1 \cup D2$, and $t' \geq \tau$ then $\mathbf{x}(t) \in D1 \cup D2, t \in [t_0 - \tau, t_0]$,

therefore $\mathbf{x}(t_0 - \tau) \in D1 \cup D2$ and from the switching rules (36) $j = 1$ and $i = 1$ ($\mathbf{x}(t_0) \in D1$) or $i = 2$ ($\mathbf{x}(t_0) \in D2$), which give the matrices $\mathbf{A}_{11}$ or $\mathbf{A}_{21}$. S2: If $\mathbf{x}(t_0) \in D3$ and $t' \leq \tau$, then from the restriction on $f_0$ $\mathbf{x}(t) \in D3, t \in (t_0 - t', t_0]$, and $\mathbf{x}(t) \in D1 \cup D2, t \in [t_0 - \tau, t_0 - t']$. Therefore $\mathbf{x}(t_0 - \tau) \in D1 \cup D2$ and from the switching rules (36), the linear system defined by $\mathbf{A}_{21}$ must be used in $D3$. Starting scenario $S_3$ can be proved similar to $S_1$ and $S_4$ to $S_2$. ∎

For $S_4$ and $S_2$, some of the initial conditions $\mathbf{x}(t_0) \in D1 \cup D2$ and $\mathbf{x}(t_0) \in D3$ are inconsistent with the definition of $S_4$ and $S_2$, respectively. Since the definitions of $S_4$ and $S_2$ includes that $\mathbf{x}(t_0 - t') \in S^D$, $t' < \tau$, for $S_4$, or $t' \leq \tau$, for $S_2$, only initial conditions $\mathbf{x}(t_0)$ that can be reached from $S^D$ (within $t'$ minutes without passing $S^D$ again) are consistent with the definition. In order to exclude $\mathbf{x}(t_0)$ which can not be reached, we need to find out what linear systems that have been used during the time period before $t_0$ i.e. when $t \in [t_0 - t', t_0)$.

**Lemma 2.** *During the time period* $t \in [t_0 - t', t_0)$, *if* $t' < \tau$ *and* $\mathbf{x}(t) \in D1 \cup D2$ *then* $\mathbf{A}_{12}$ *(*$\mathbf{x}(t) \in D1$*) or* $\mathbf{A}_{22}$ *(*$\mathbf{x}(t) \in D2$*) is used. If* $t' \leq \tau$ *and* $\mathbf{x}(t) \in D3$ *then* $\mathbf{A}_{21}$ *is used.*

*Proof:* If $\mathbf{x}(t_0) \in D1 \cup D2$, then, by the definition of $t'$, $\mathbf{x}(t) \in D1 \cup D2$ only, during $t \in [t_0 - t', t_0)$, then by the restriction on $f_0$, $\mathbf{x}(t) \in D3$ only, during $t \in [(t_0 - \tau), (t_0 - t'))$, and also $\mathbf{x}(t) \in D3$ only, during $t \in [((t_0 - t') - \tau), (t_0 - \tau))$. Therefore, by the switching rules (36), $j = 2$, the corresponding time period

$\tau$ minutes later, i.e. when $t \in [(t_0 - t'), t_0)$ and $\mathbf{A}_{12}$ ($\in D1$) or $\mathbf{A}_{22}$ ($\in D2$) is used. A similar argument can be used for $\mathbf{A}_{21} \in D3$. ∎

As an example of inconsistent initial values, consider $S_4$. By lemma 2 for $t \in [t_0 - t', t_0)$ only $\mathbf{A}_{22} \in D2$ or $\mathbf{A}_{12} \in D1$ is used (corresponding to the vector fields of Fig. 7*c*). The region of $D2$ which is shadowed in Fig. 7*c* can, from the figure, not be reached from $S^D$ by the use of the linear systems $\mathbf{A}_{22}$ and $\mathbf{A}_{12}$. A similar phenomena is observed for $S_2$, which excludes a region of $D3$ where the vector field points towards $S^D$.(This region is too small to be seen in Fig. 7*b*.)

Next, from the vector fields of Fig. 7 together with the information on whether there will be a delayed switch or not, we conclude that a trajectory can only follow the movement chart $S_1 \rightarrow S_2 \rightarrow S_3 \rightarrow S_4 \rightarrow S_1$, i.e. from figure $a$ to $b$ to $d$ to $c$ and back to $a$.

**Lemma 3.** *For $M = 1.8$ any trajectory satisfying the restriction on $f_0$ must move according to $S_1 \rightarrow S_2 \rightarrow S_3 \rightarrow S_4 \rightarrow S_1$.*

*Proof:* The proof is based on Fig. 7. A trajectory starting in $S_1$, i.e. in $a$ of Fig. 7, has been on the left side of the delayed switching line ($\in D1 \cup D2$) the last $\tau$ minutes. Thus, there cannot be a delayed switch to another system. Therefore, the trajectory has to follow the vector field of $a$ until it moves to $D_3$ and $S_2$. Since a trajectory initiating from $S_2$ has passed $S^D$ the last $\tau$ minutes, there has to be a delayed switch to another system within $\tau$ minutes. Until then the only possibility for a trajectory is to move closer to the fixed

point. The delayed switch means that the trajectory moves to $S_3$ and Fig. 7*d*. When in $S_3$, it was more than $\tau$ minutes, since the last time $S^D$ was passed. Hence, there is no delayed switch. Then, the only possibility is that the trajectory moves to $D2$, and thus scenario $S_4$, i.e. Fig. 7*c*. Now, it was less than $\tau$ minutes since $S^D$ was passed. Then there will be a delayed switch within $\tau$ minutes. The only possibility until then is that the trajectory moves closer to the fixed point. When the delayed switch takes place the system is back in $S_1$ and Fig. 7*a*. ∎

By this we have proved that for $M = 1.8$ any trajectory has to move according to $S_1 \to S_2 \to S_3 \to S_4 \to S_1$ as time increase. One notes here that a trajectory that moves according to this cannot pass $S^D$ more than once during $\tau$ minutes. Hence the restriction on $\mathbf{f}_0$ will always be satisfied.

**Lemma 4.** *For $M = 1.8$, a trajectory that moves according to $S_1 \to S_2 \to S_3 \to S_4 \to S_1$ must approach a globally stable limit cycle as $t$ increases.*

*Proof:* By Fig. 7, any trajectory that passes from $S_2 \to S_3 \to S_4$ must reach the slow fp-eigenvector in $D2$ of $S_4$. When this fp-eigenvector is reached $t' = 0$. The time it takes to follow the slow fp-eigenvector into $D1$ is $< \tau$. Thus, $D1$ of $S_4$ must be reached. By Fig. 7 *c*, a trajectory that reach $D1$ of $S_4$ from the slow fp-eigenvector in $D2$ of $S_4$, must reach the slow fp-eigenvector in $D1$ of $S_1$. A trajectory following the slow fp-eigenvector in $D1$ of $S_1$ must traverse $S^I$ at a uniquely defined point (The point were the slow fp-eigenvector in $D1$ of $S_1$ traverses $S^I$.). When this happens $t' > \tau$ by the

definition of $S_1$. Thus there is no delayed switches initiated. The solution is thereby uniquely defined. ∎

Now we have proved that for $M = 1.8$ there exist a limit cycle, which is globally stable under the restriction on $f_0$. Next we need to consider what happens for other values of $M$. The fixed points and thus the slow fp-eigenvectors are the only things that are changed in Fig. 7 when $M$ varies. Since the fast eigenvectors all are $(0, 1)$, they are independent of $M$. In Fig. S10, is plotted the fixed points as a function of $M$, i.e. $\hat{\mathbf{x}}_{ij}(M)$ for $M_{min} < M < M_{max}$, where $M_{min} = 0.8$ and $M_{max} = 3$, for the four linear systems. Here is also shown the slow fp-eigenvectors $\mathbf{v}_1(M_{min})$ and $\mathbf{v}_1(M_{max})$. Thus, we have seen that for these values of $M$, the only change in the vector field that can give a qualitative change of system dynamics is the position of $\hat{\mathbf{x}}_{11}(M)$ (thick line in Fig. S10$a$). For small $M < 1.66$, $\hat{\mathbf{x}}_{11}(M)$ is in $D1$ and for larger $M > 1.66$ $\hat{\mathbf{x}}_{11}(M)$ is in $D2 \cup D3$. If $M > 1.66$ then, from this figure and the reasoning above, we see that the only possibility is to move according to $S_1 \to S_2 \to S_3 \to S_4 \to S_1$. When $M < 1.66$ the only possibility is to move according to $S_2 \to S_3 \to S_4 \to S_1$ and any trajectory will approach $\hat{\mathbf{x}}_{11}$ as time increase. This concludes the proof of the stability theorem.

## References


[1] Novak, B., Pataki, Z., Ciliberto, A., and Tyson, J. J.: 'Mathematical model of the cell division cycle of fission yeast'. *Chaos*, 2001, **11**, pp. 277–286

[2] Goldbeter, A. and Koshland, D. E. J.: 'An amplified sensitivity arising from covalent modification in biological systems'. *Proc. Natl. Acad. Sci. U S A.*, 1981, **78**, pp. 6840–6844

[3] Tyson, J. J., Chen, J. C., and Novak, B.: 'Sniffers, buffers, toggles and blinkers: dynamics of regulatory and signaling pathways in the cell'. *Curr. Opin. Cell. Biol.*, 2003, **15**, pp. 221–231

Fig. S1: *Variable dependencies of the original model and subdivision into switching modules.*

Graph of variable dependencies. A node corresponds to a state-variable of the NT-model, (1)-(17). There is an edge from node $j$ to $i$ if $j$ is on the right hand side of an equation defining $i$. Arrows $i \to i$ are not included.

*a* Full DPL-model, subdivision into switching modules when $M \geq 0$.

*b* Small DPL-model, subdivision into switching modules when $M > 0.8$. Some of the variables can be replaced by constant parameters (indicated by crosses), when $M > 0.8$.

Fig. S2: *Steady-state input/output behaviour of* $M_{25}$, $M_{\mathrm{wee}}$ *and* $M_{\mathrm{slp}}$ *and derivation of step-function parameters.*

The solid lines corresponds to the functions $f^{ss}_{k_{25}}$ (equation 14), $f^{ss}_{k_{\mathrm{wee}}}$ (equation 13) and $f^{ss}_{M_{\mathrm{slp}}}$ respectively. The input/output function $f^{ss}_{M_{\mathrm{slp}}}$ is retrieved by solving the equations (4-6), with $\frac{d[\mathrm{Slp1_T}]}{dt} = 0$, $\frac{d[\mathrm{Slp1}]}{dt} = 0$ and $\frac{d[\mathrm{IEP}]}{dt} = 0$, for $[\mathrm{Slp1_T}], [\mathrm{Slp1}]$ and [IEP], respectively, while only considering biological possible solutions. Then $f^{ss}_{M_{\mathrm{slp}}}$ is given by successive variable elimination. The dashed lines refer to the corresponding fine-tuned step functions.

Fig. S3: *Steady-state input/output behaviour of* $M_{\mathrm{sk}}$ *and derivition of step-function parameters.*

*a* The function $f^{ss}_{M_{\mathrm{sk}}}$, which is retrived by solving equation (8), with $\frac{d[\mathrm{SK}]}{dt} = 0$ for [SK] and next insert equation (12).

*b* The corresponding step function.

Fig. S4: *Steady-state input/output behaviour of* $M_{\text{ste}}$ *and derivation of step-function parameters.*

The solid lines corresponds to the function $f^{ss}_{[\text{Ste9}]}([\text{MPF}], [\text{Slp1}], [\text{SK}])$, and the four figures correspond to the four combinations $f^{ss}_{[\text{Ste9}]}([\text{MPF}], [\text{Slp1}] \in \{\text{h}_{\text{slp}}, \text{l}_{\text{slp}}\}, [\text{SK}] \in \{\text{h}_{\text{sk}}, \text{l}_{\text{sk}}\})$. These are retrieved by solving equation (3), with $\frac{d[\text{Ste9}]}{dt} = 0$, for [Ste9], while only considering biological possible solutions. The solution corresponds to the Goldbeter-Koshland function (16), i.e. $f^{ss}_{[\text{Ste9}]}([\text{MPF}], [\text{Slp1}], [\text{SK}]) = G((k'_3 + k''_3[\text{Slp1}]), (k'_4[\text{SK}] + k_4[\text{MPF}]), J_3, J_4)$. The dashed lines shows the corresponding fine-tuned step functions.

Fig. S5: *Steady-state input/output behaviour of* $M_{\mathrm{rum}}$ *and derivation of step-function parameters.*

The solid lines corresponds to the function $f^{ss}_{[\mathrm{Rum1_T}]}([\mathrm{MPF}], [\mathrm{SK}] = \mathrm{l_{sk}})$ (left) and $f^{ss}_{[\mathrm{Rum1_T}]}([\mathrm{MPF}], [\mathrm{SK}] = \mathrm{h_{sk}})$ (right). These functions are retrieved by solving equation (7), with $\frac{d[\mathrm{Rum1_T}]}{dt} = 0$, for $[\mathrm{Rum1_T}]$. The dashed lines shows the corresponding fine-tuned step functions.

Fig. S6: *Estimation of time-delay.* The input/output step-response of the different subsystems. The dashed line corresponds to the step-wise changing input.

*a* Subsystem $M_{\mathrm{slp}}$. The label on the y-axis, [Slp1]([MPF]), denotes the response of output [Slp1] (solid line) to input [MPF] (dashed). [MPF] is changed from 0 to 1.5 and back.

*b-c* Subsystem $M_{\mathrm{sk}}$.

*d-f* Subsystem $M_{\mathrm{ste}}$.

*g-h* Subsystem $M_{\mathrm{rum}}$.

Fig. S7: *Validation of the small DPL-model for several initial conditions.* Numerical simulations with the NT-model (left) and the DPL-model (right) for different initial conditions. Each row corresponds to one comparison of simulations starting with the same initial condition (see text). Dashed-dotted line corresponds to M, dashed line to [MPF] (NT-model) or $y_{\mathrm{MPF}}$ (DPL-model) and solid line to SlpSte (NT) or $s_{\mathrm{slp/ste}}$ (DPL).

Fig. S8: See Figure S7.

Fig. S9: See Figure S7.

Fig. S10: *Illustration to the proof on the theorem of stability, see Supplementary material S4.*

The fixed points $\hat{\mathbf{x}}_{ij}(M)$ for $M_{min} < M < M_{max}$, where $M_{min} = 0.8$ and $M_{max} = 3$ and the slow fp-eigenvectors $\mathbf{v}_1(M_{min})$ and $\mathbf{v}_1(M_{max})$, for the four different linear systems. For $A_{21}$, $A_{12}$ and $A_{22}$ $\mathbf{v}_1(M_{min})$ and $\mathbf{v}_1(M_{max})$ are overlapping. The fast eigenvectors (not shown) are all vertical $(0, 1)$ and independent of $M$. No distinction between bona-fide and virtual fixed points is made in the figure.

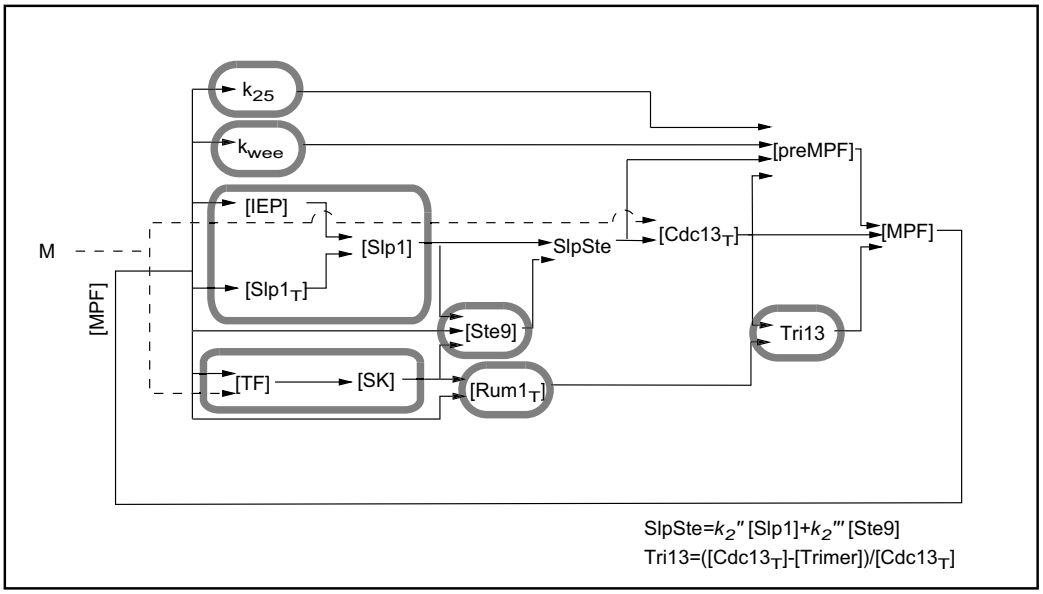
k25
kwee
[preMPF]
[IEP]
[Slp1]
SlpSte
[Cdc13T]
[MPF]
M
[MPF]
[Slp1T]
[Ste9]
Tri13
[TF]
[SK]
[Rum1T]
SlpSte=k2''[Slp1]+k2'''[Ste9]
Tri13=([Cdc13T]-[Trimer])/[Cdc13T]

*a*

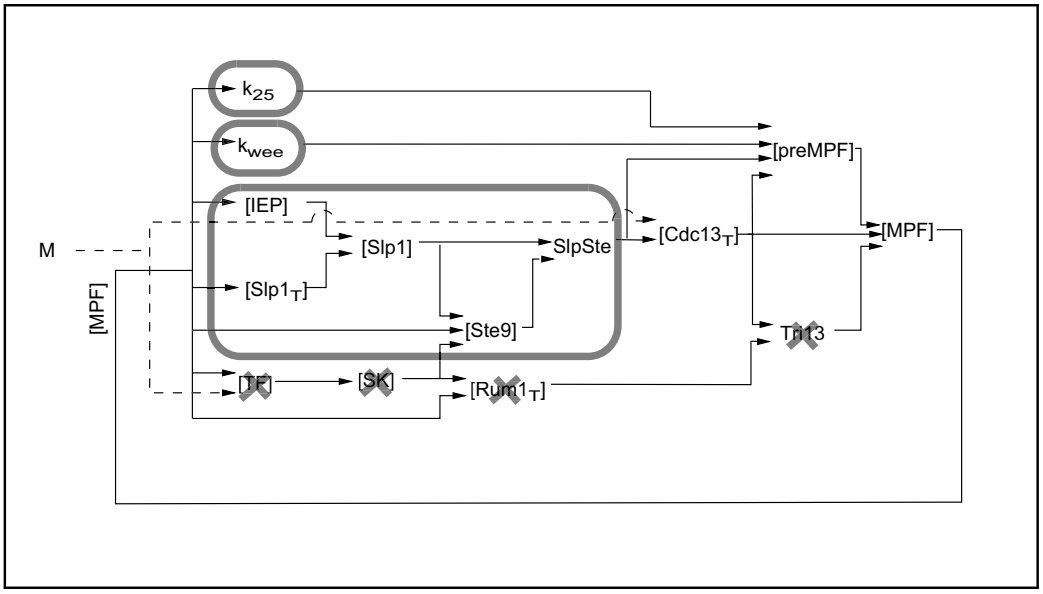
k25
kwee
[preMPF]
[IEP]
[Slp1]
SlpSte
[Cdc13T]
[MPF]
M
[MPF]
[Slp1T]
[Ste9]
Tri13
[TF]
[SK]
[Rum1T]

*b*

Fig. S1:

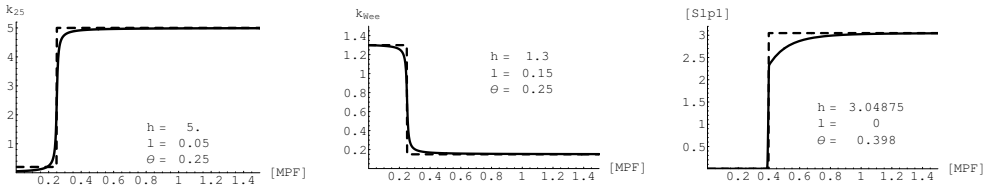
k25
5
4
3
2
1
h = 5.
l = 0.05
Θ = 0.25
0.2 0.4 0.6 0.8 1 1.2 1.4
[MPF]
kWee
1.4
1.2
1
0.8
0.6
0.4
0.2
h = 1.3
l = 0.15
Θ = 0.25
0.2 0.4 0.6 0.8 1 1.2 1.4
[MPF]
[Slp1]
3
2.5
2
1.5
1
0.5
h = 3.04875
l = 0
Θ = 0.398
0.2 0.4 0.6 0.8 1 1.2 1.4
[MPF]

Fig. S2:

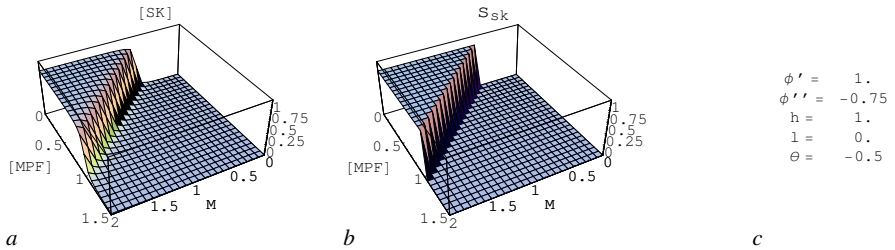


*a* *b* *c*

Fig. S3:

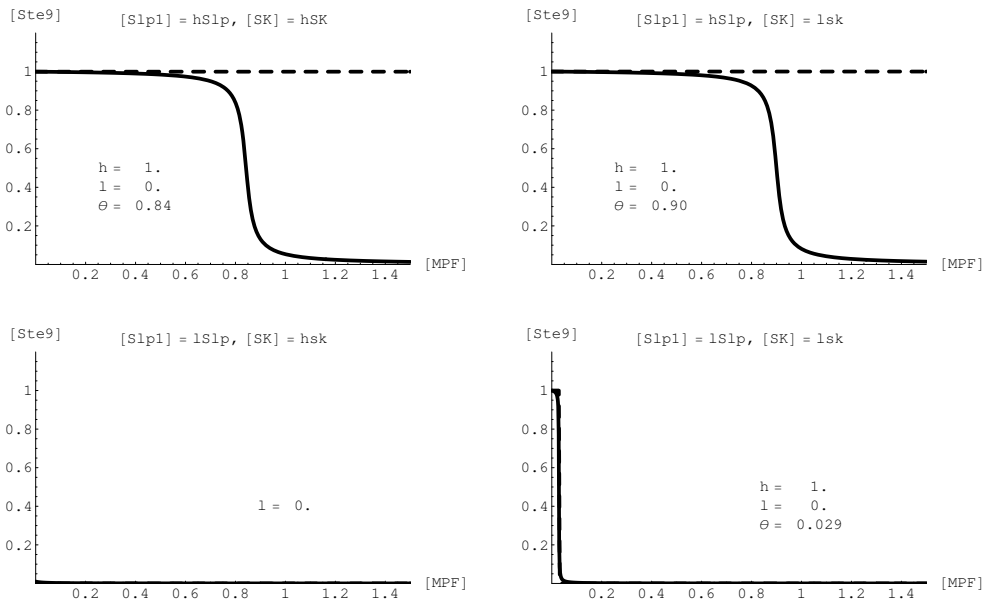
[Ste9]
[Slp1] = hSlp, [SK] = hSK
h = 1.
l = 0.
θ = 0.84
[MPF]
[Ste9]
[Slp1] = hSlp, [SK] = lsk
h = 1.
l = 0.
θ = 0.90
[MPF]
[Ste9]
[Slp1] = lSlp, [SK] = hsk
l = 0.
[MPF]
[Ste9]
[Slp1] = lSlp, [SK] = lsk
h = 1.
l = 0.
θ = 0.029
[MPF]

Fig. S4:

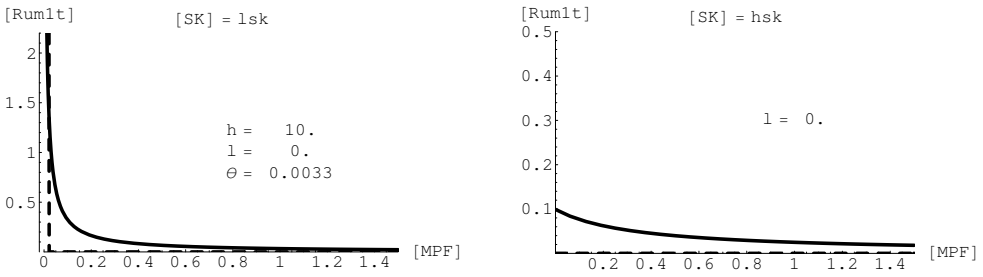


Fig. S5:

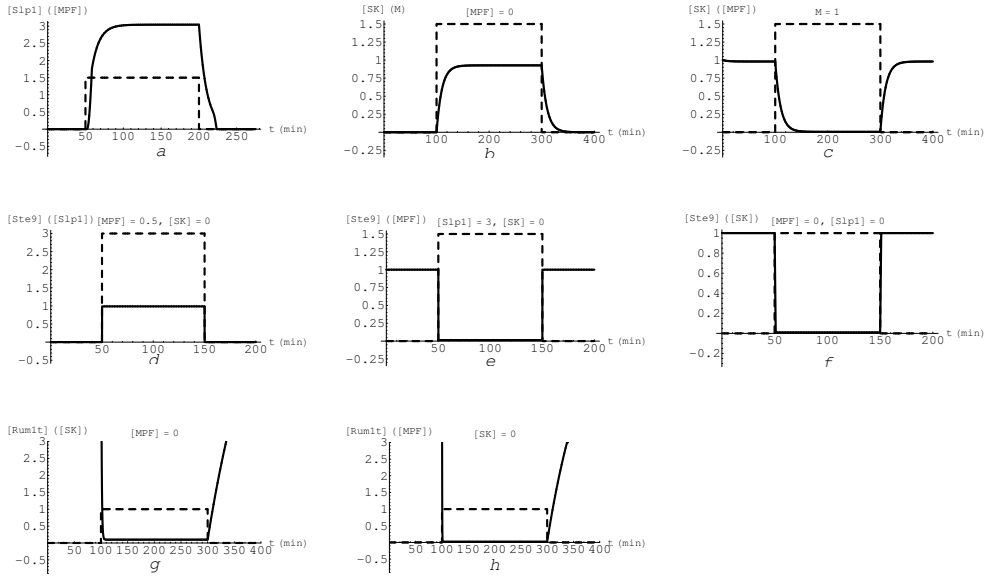
[Slp1] ([MPF])
t (min)
a
[SK] (M)
[MPF] = 0
t (min)
b
[SK] ([MPF])
M = 1
t (min)
c
[Ste9] ([Slp1])
[MPF] = 0.5, [SK] = 0
t (min)
d
[Ste9] ([MPF])
[Slp1] = 3, [SK] = 0
t (min)
e
[Ste9] ([SK])
[MPF] = 0, [Slp1] = 0
t (min)
f
[Rum1t] ([SK])
[MPF] = 0
t (min)
g
[Rum1t] ([MPF])
[SK] = 0
t (min)
h

Fig. S6:

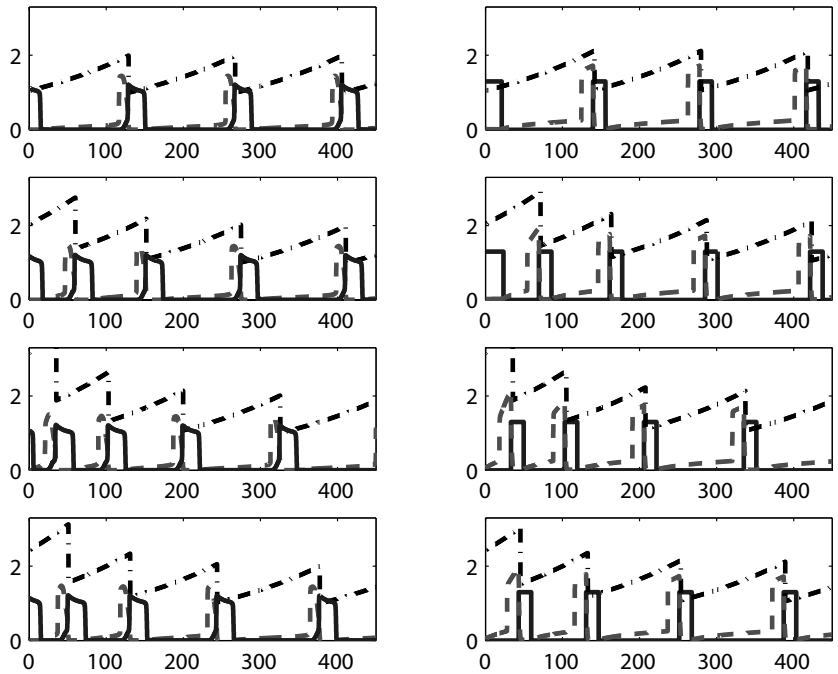


Fig. S7:

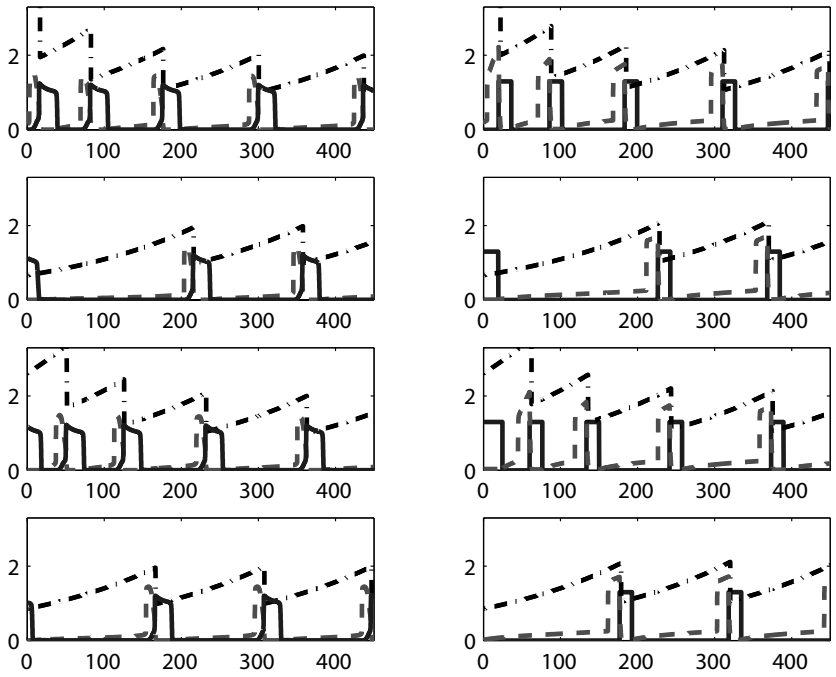


Fig. S8:

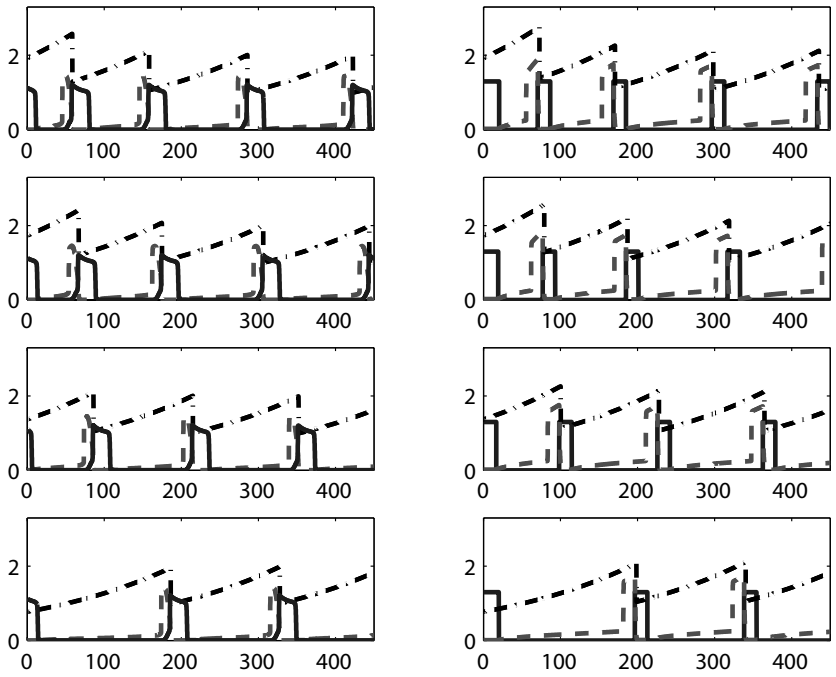


Fig. S9:

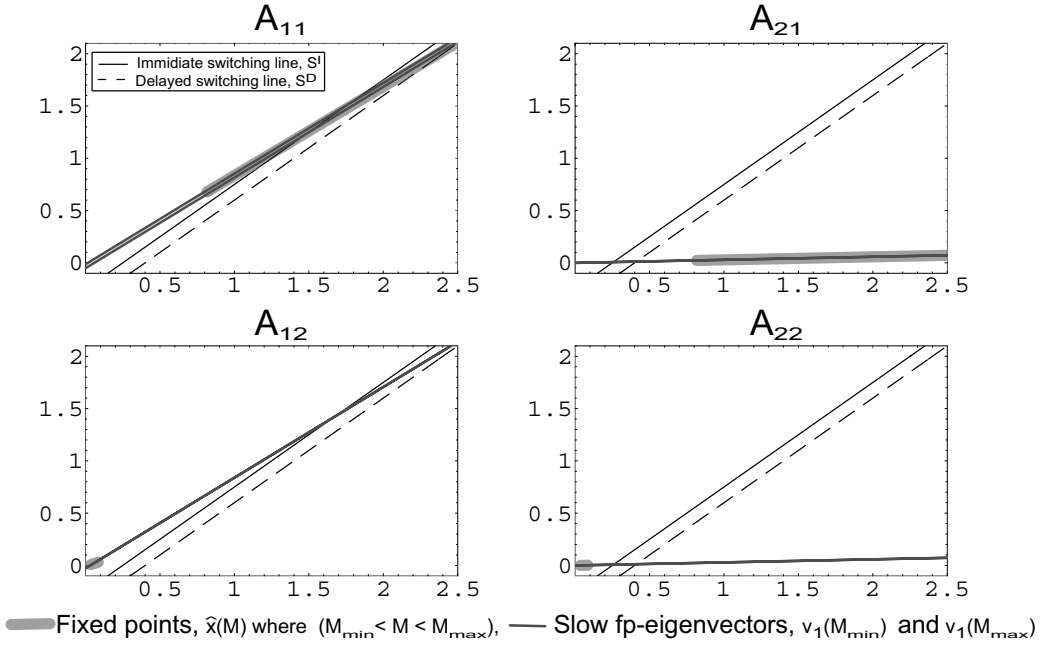
A11
A21
A12
A22
Immidiate switching line, S^I
Delayed switching line, S^D
Fixed points, x̂(M) where (M_min < M < M_max),
Slow fp-eigenvectors, v1(M_min) and v1(M_max)

Fig. S10:

| | Parameter changes |
|---|---|
| strains | NT |
| WT | - |
| $wee1^{ts}$ | $k''_{wee} = 0.3$ |
| $wee1\Delta$ | $k'_{wee} = k''_{wee} = 0$ |
| $cdc25\Delta$ | $k'_{25} = k''_{25} = 0.02$ |
| $wee1^{ts}cdc25\Delta$ | $k'_{25} = k''_{25} = 0.02, k''_{wee} = 0.3$ |
| $wee1\Delta cdc25\Delta$ | $k'_{25} = k''_{25} = 0.02, k'_{wee} = k''_{wee} = 0$ |
| $rum1t\Delta$ | $d[\mathrm{Rum1_T}]/dt = 0, [\mathrm{Rum1_T}](t_0) = 0$ |
| $rum1t\Delta wee1^{ts}$ | $d[\mathrm{Rum1_T}]/dt = 0, [\mathrm{Rum1_T}](t_0) = 0, k''_{wee} = 0.3$ |
| $ste9\Delta$ | $d[\mathrm{Ste9}]/dt = 0, [\mathrm{Ste9}](t_0) = 0$ |
| $ste9\Delta wee1^{ts}$ | $d[\mathrm{Ste9}]/dt = 0, [\mathrm{Ste9}](t_0) = 0, k''_{wee} = 0.3$ |
| $ste9\Delta rum1t\Delta$ | $d[\mathrm{Ste9}]/dt = 0, [\mathrm{Ste9}](t_0) = 0,$ $d[\mathrm{Rum1_T}]/dt = 0, [\mathrm{Rum1_T}](t_0)=0$ |
| $ste9\Delta rum1t\Delta wee1^{ts}$ | $d[\mathrm{Ste9}]/dt = 0, [\mathrm{Ste9}](t_0) = 0,$ $d[\mathrm{Rum1_T}]/dt = 0, [\mathrm{Rum1_T}](t_0) = 0, k''_{wee} = 0.3$ |
| strains | DPL |
| WT | - |
| $wee1^{ts}$ | $h_{wee} = 0.3$ |
| $wee1\Delta$ | $h_{wee} = l_{wee} = 0$ |
| $cdc25\Delta$ | $h_{25} = l_{25} = 0.02$ |
| $wee1^{ts}cdc25\Delta$ | $h_{25} = l_{25} = 0.02, l_{wee} = 0.3$ |
| $wee1\Delta cdc25\Delta$ | $h_{25} = l_{25} = 0.02, l_{wee} = h_{wee} = 0$ |
| $rum1t\Delta$ | $h_{\mathrm{rum}} = l_{\mathrm{rum}} = 0$ |
| $rum1t\Delta wee1^{ts}$ | $h_{\mathrm{rum}} = l_{\mathrm{rum}} = 0, h_{wee} = 0.3$ |
| $ste9\Delta$ | $h_{\mathrm{ste}} = l_{\mathrm{ste}} = 0$ |
| $ste9\Delta wee1^{ts}$ | $h_{\mathrm{ste}} = l_{\mathrm{ste}} = 0, h_{wee} = 0.3$ |
| $ste9\Delta rum1t\Delta$ | $h_{\mathrm{ste}} = l_{\mathrm{ste}} = 0, h_{\mathrm{rum}} = l_{\mathrm{rum}} = 0$ |
| $ste9\Delta rum1t\Delta wee1^{ts}$ | $h_{\mathrm{ste}} = l_{\mathrm{ste}} = 0, h_{\mathrm{rum}} = l_{\mathrm{rum}} = 0, h_{wee} = 0.3$ |

Table S1: Parameter changes of the mutated strains of table 1. All changes are relative the WT (wild-type) cell (equations (1-18)). The values $k'_{25} = k''_{25} = 0.02$ and $k''_{wee} = 0.3$ are taken from [1].